The 9th European Congress on Computational Methods in Applied Sciences and Engineering
ECCOMAS Congress 2024
3 – 7 June 2024, Lisboa, Portugal

A DISPLACEMENT-BASED DESIGN PROCEDURE OF HYSTERETIC DISSIPATIVE STEEL EXOSKELETONS FOR THE SEISMIC RETROFITTING OF RC HOSPITAL BUILDINGS

FABIO MAZZA[*] AND DOMENICO RIZZO[†]

[*] Dipartimento di Ingegneria Civile
Università della Calabria
Ponte P. Bucci, 87036 Rende (Cosenza), Italy
e-mail: fabio.mazza@unical.it

† Dipartimento di Architettura, Costruzione e Design
Politecnico di Bari
Via Orabona 4, 70125 Bari, Italy
email: domenico.rizzo@uniba.it

Key words: RC framed structure, Steel exoskeleton, Hysteretic damper, Displacement-based design procedure, Nonlinear seismic analysis.

Summary. One of the primary challenges in the seismic retrofitting of hospital buildings lies in the research of an effective solution so as not to interrupt their ability to provide a much-needed service. To this aim, the use of dissipative steel exoskeletons (DEXs), placed in parallel to the façades of the existing structure and equipped with their own foundation, represents a viable technique. A displacement-based design (DBD) procedure of DEXs made of concentric braced frames and hysteretic dampers is proposed in the present work, looking at substantially limit structural as well as non-structural damage of the existing framed building (F). Attention is focused on the in-plane (IP) and out-of-plane (OOP) nonlinear response of masonry infills (MIs). A five-storey reinforced concrete (RC) pavilion of the hospital campus in Avellino (Italy), with MIs placed in the interior bays of the perimeter frames, is considered as case study and retrofitted with hysteretic DEXs in a high-risk seismic zone. Three external arrangements of DEXs parallel to all façades of the existing building are selected: i.e. lumped (DEX.L) and distributed (DEX.D), placed along some (with MIs) or all perimetral bays, respectively; mixed (MDEX.L), where DEX.L is combined with a steel EX parallel to the corner perimetral bays. A lumped plasticity model is adopted for RC frame members, while a five-element macro-model is considered for MIs. Elastic-linear behaviour is assumed for steel frame members of the DEXs, while hysteretic damped braces are modelled with truss elements characterised by a bilinear force-displacement law. The retrofit target displacement is derived from the capacity curve of the original bare structure, assuming linear and uniform vertical distributions of the seismic load. This is followed by nonlinear dynamic analysis of the infilled structure before and after retrofitting, in which IP and OOP contributions of MIs parallel and perpendicular to the direction of seismic loads, respectively, are considered. The effectiveness and reliability of the proposed DBD procedure of hysteretic DEXs is checked at the at the serviceability and ultimate design earthquakes.

1 INTRODUCTION

In recent years, considerable attention has been paid to seismic retrofitting strategies based on use of dissipative exoskeletons (DEXs) carried out from the outside of the building, hence resulting particularly suitable for public buildings such as hospitals [1], schools [2] and airports [3]. This type of solution limits the interference with the building's functionality and interacts with the primary structure only at the floor levels where rigid or dissipative links are placed, while an own foundation avoids the need of local strengthening of columns and foundations. Parallel and orthogonal arrangement of DEXs to the façades of the building are generally used for steel bracing systems eventually equipped with dissipative devices placed between adjacent floors or located at the base [4]. Different design procedures of DEXs are aimed at reducing seismic demand of structural members and preventing in-plane (IP) collapse of non-structural masonry infills (MIs), combining linear [1, 5] and nonlinear [6] behaviour of exoskeleton's steel members and selected supplemental damping solution. However, the out-of-plane (OOP) collapse of MIs is not taken into account, although high OOP vulnerability and IP-OOP mutual interaction are frequently observed [7].

The aim of the present work is the proposal of a displacement-based design (DBD) procedure of DEXs, constituted of an elastic steel exoskeleton equipped with hysteretic damped braces (HYDBs) and rigidly coupled to the original structure that needs to be retrofitted. A five-storey reinforced concrete (RC) pavilion of the hospital campus of Avellino (Italy), characterized by MIs placed in the interior bays of the perimeter frames, is considered as case-study [8]. Firstly, nonlinear static analysis of the original (bare) structure with nonstructural MIs, designed in compliance with a former Italian building code (DM96) for a medium-risk seismic zone [9], is carried out for the assessment of its seismic vulnerability. Then, three common layouts of DEXs placed in parallel position to all façades of the existing building are designed to meet the requirements of the current Italian building code (NTC18) in a high-risk seismic zone [10]: i.e. lumped along bays with MIs (DEX.L), to improve the functionality of the openings; distributed along all bays (DEX.D), to increase their redundancy; mixed (MDEX.L), where DEX.L is combined with a steel EX parallel to the corner perimetral bays. A homemade computer code is implemented for nonlinear dynamic analysis of the original (F) and retrofitted (DEXF) infilled frames [7, 8]. To this end, artificial accelerograms are generated [11], whose response spectra match serviceability and ultimate design response spectra adopted by NTC18.

2 DISPLACEMENT-BASED DESIGN PROCEDURE OF THE DEX

A four-step displacement-based design (DBD) procedure of an external steel concentric bracing systems equipped with hysteretic dampers is proposed, starting from the parallel rigid coupling of two equivalent single-degree-of-freedom (SDOF) systems representative of the original frame (F) and dissipative exoskeleton (DEX). Note that the DBD procedure involves two external (see steps 2-3 and 2-4) and one internal (see step 4) iteration loops related to equivalent viscous damping ($\xi_{e,DEXF}$), mass (α_m) and stiffness (α_k) unknown ratios.

2.1 Properties of the SDOF system equivalent to the original frame

The force-displacement curve of the equivalent SDOF system ($V^*(=V_F/\Gamma)$-$d^*(=d/\Gamma)$, being Γ the coefficient of participation of the first vibration mode) is first derived, starting from the

base shear (V_F) versus roof-storey displacement (d) capacity curve of the original framed structure, and then idealized as bilinear assuming a stiffness hardening ratio r_F. Once the displacement corresponding to a selected performance displacement (d^*_p) is fixed, the equivalent (secant) stiffness can be evaluated for the frame

$$K_{e,F} = \frac{V^*_{p,F}}{d^*_p} \tag{1}$$

being $V^*_{p,F}$ the base shear at the performance displacement. Afterwards, the equivalent viscous damping due to hysteresis $\xi_{h,F}$ can be calculated

$$\xi_{h,F} = \kappa \frac{63.7(\mu_F - 1)(1 - r_F)}{\mu_F[1 + r_F(\mu_F - 1)]} \tag{2}$$

as function of the following parameters: ductility demand $\mu_F (=d^*_p/d^*_{y,F}=d_p/d_{y,F}$, being $d_{y,F}$ the yield displacement); reduction factor κ(=0.33, depending on the degrading response of RC frame members).

2.2 Properties of the SDOF system equivalent to the hysteretic dissipative exoskeleton

On the basis of an initial (tentative) value of the mass ratio ($\alpha_m^{(0)}$), the effective mass of DEXF is obtained

$$m_{e,DEXF} = \left(1 + \alpha_m{}^{(0)}\right) \cdot m_{e,F} = \left(1 + \alpha_m{}^{(0)}\right) \cdot \sum_{i=1}^{n} \left(m_{i,F} \cdot \phi_i\right) \tag{3}$$

as function of the effective mass of the SDOF system equivalent to the original frame evaluated by multiplying the first-mode (horizontal) components (ϕ_1, ϕ_2, .., ϕ_n) by the corresponding floor masses ($m_{1,F}$, $m_{2,F}$, .., $m_{n,F}$). Then, the effective stiffness of DEXF is evaluated with reference to the acceleration design value (a^*_p)

$$K_{e,DEXF} = \frac{m_{e,DEXF} \cdot a^*_p}{d^*_p} \tag{4}$$

the latter resulting from the displacement-acceleration design response spectra corresponding to an initial (tentative) value of the equivalent viscous damping ratio of DEXF ($\xi^{(0)}_{DEXF}$). Then, the effective stiffness required to DEX is evaluated as

$$K_{e,DEX} = K_{e,DEXF} - K_{e,F} \tag{5}$$

Since the force-displacement curve of the DEX is idealized as bilinear, the base-shear at the performance and yielding points can be calculated as

$$V^*_{p,DEX} = K_{e,DEX} \cdot d^*_p \tag{6a}$$

$$V^*_{y,DEX} = \frac{V^*_{p,DEX}}{1 + r_{DEX} \cdot (\mu_{DEX} - 1)} \tag{6b}$$

as function of the equivalent ductility demand of DEX

$$\mu_{DEX} = 1 + \frac{(\mu_D - 1)(1 + r_{DEX}K^*_D)}{1 + K^*_D} = \mu_D, \text{for } K^*_D = \frac{K_D}{K_{DB}} = 0 \tag{7}$$

and the equivalent stiffness hardening ratio of DEX

$$r_{DEX} = \frac{r_D(1+K_D^*)}{1+r_D\,K_D^*} = r_D, \text{for } K_D^* = \frac{K_D}{K_{DB}} = 0 \tag{8}$$

being μ_D and r_D the ductility demand and hardening ratio of the equivalent hysteretic damper, respectively.

Finally, the equivalent viscous damping ratio due to hysteresis of the DEX can be evaluated by one of the following expressions [12]

$$\xi_{h,DEX} = \left[85 + 60(1 - T_{e,DEXF})\right]\frac{\mu_{DEX}-1}{\pi\mu_{DEX}}, \text{for } \mu_{DEX} > 1 \text{ and } T_{e,DEXF} < 1s \tag{9a}$$

$$\xi_{h,DEX} = 85\frac{\mu_{DEX}-1}{\pi\mu_{DEX}}, \text{for } \mu_{DEX} > 1 \text{ and } T_{e,DEXF} \geq 1s \tag{9b}$$

where the effective period of DEXF is calculated as

$$T_{e,DEXF} = 2\pi\sqrt{\frac{m_{e,DEXF}}{K_{e,DEXF}}} \tag{10}$$

2.3 Equivalent viscous damping of the frame with hysteretic dissipative exoskeleton

Assuming a suitable value of the elastic viscous damping ratios for the framed structure (e.g. $\xi_{v,F}$=5%) and steel exoskeleton (e.g. $\xi_{v,EX}$=2%), the equivalent viscous damping ratio of DEXF is derived from the expression:

$$\xi_{e,DEXF} = \xi_{v,F} + \xi_{v,EX} + \frac{\xi_{h,F}V_{p,F}^* + \xi_{h,DEX}V_{p,DEX}^*}{V_{p,F}^* + V_{p,DEX}^*} \tag{11}$$

where $\xi_{h,F}$ and $\xi_{h,DEX}$ are calculated in Sections 2.1 and 2.2, respectively. It is worth to note that the equivalent viscous damping ratio expressed by the Equation (11) depends on the base-shear $V^*_{p,DEX}$, which is initially unknown. As a consequence, an iterative procedure is needed for the solution of Equations (4)-(11).

2.4 Properties of the hysteretic dissipative exoskeleton for the actual structure

The proportional stiffness criterion, that assumes a constant stiffness ratio (i.e. α_k=K_{DEX}/K_F, for DEX.L and DEX.D, and α_k=($K_{(M)DEX}$+ K_{EX})/K_F, for MDEX.L) along the building height, is used to evaluate stiffness and strength design properties of the hysteretic DEX. Specifically, the distribution of the lateral loads resulting from the first-mode shape (i.e., ϕ_i=$\phi_{i,F}$=$\phi_{i,EX}$=$\phi_{i,DEX}$, i =1,..,n) of the original structure, that remains practically unchanged after the insertion of the DEX, is considered

$$K_{i,DEX} = \frac{V_{yi,DEX}}{(\phi_i - \phi_{i-1})\cdot d_{y,DEX}} \tag{12a}$$

$$V_{yi,DEX} = \sum_{j=i}^{n} F_{yj,DEX} \tag{12b}$$

$$F_{yi,DEX} = \frac{m_i\phi_i}{\sum_{j=1}^{n} m_j\phi_j}V_{y,DEX} \tag{12c}$$

Then, commercial profiles of steel frame members (i.e. beams, columns and braces) of the DEX are designed and updated values of stiffness ($\alpha_k^{(1)}= V_{DEX}^{(1)}/V_F$) and mass ($\alpha_m^{(1)}$) ratios are evaluated, so requiring internal (step 4) and external (step 2-4) iterative loops, respectively. Note that, the base-shear of DEX for the MDEX.L solution is equal to

$$V_{y,(M)DEX} = V_{y,DEX} - \frac{\beta_k}{1+\beta_k} K_{DEX} \cdot d_{y,DEX} \tag{13}$$

for an assigned value of the stiffness ratio

$$\beta_k = \frac{K_{EX}}{K_{EX} + K_{(M)DEX}} \tag{14}$$

3 LAYOUT AND RETROFITTING OF A HOSPITAL BUILDING WITH DEX

The case-study hospital building shown in Figure 1 is inspired to a five-storey RC pavilion of the campus built in Avellino, Campania (Italy), where the original lengths of the longitudinal and transversal bays are modified and MIs are supposed placed in the interior bays of the perimeter frames, characterized by the lowest (i.e. $L_X/h=1.0$) and highest (i.e. $L_Y/h=1.75$) values of the aspect-ratio (i.e. width-to-height ratio). The vertical loads are represented by 7.93 kN/m^2 on the top floor and 10.23 kN/m^2 on the other floors. An additional dead load of 5.5 kN/m is assumed for the perimetral beams with MIs made of a double leaf and total thickness $t_w(=2\cdot t_{w1}$, where t_{w1}=12 cm is referred to a single leaf).

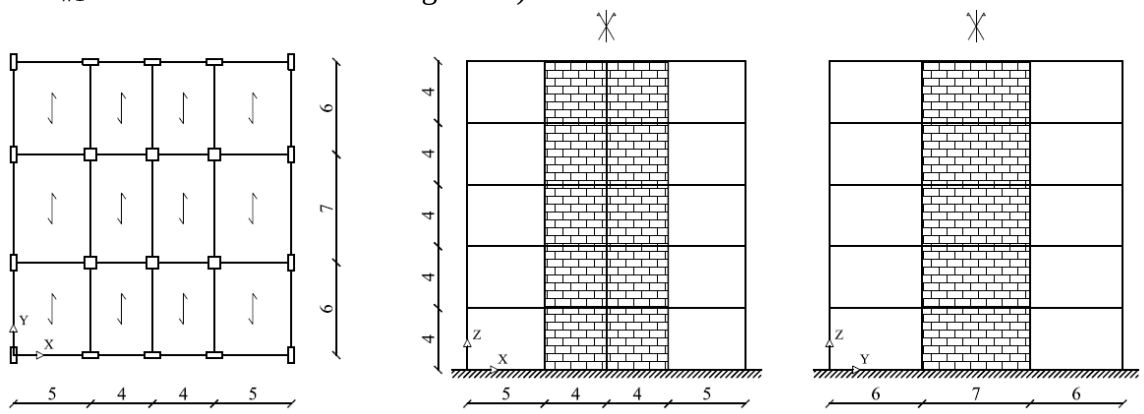

(a) Plan (X-Y) (b) Elevation (X-Z) (c) Elevation (Y-Z)

Figure 1: Layout of the original case-study hospital (unit in m)

The cylindrical compressive strength of concrete and yield strength of steel reinforcement are assumed equal 25 N/mm^2 and 450 N/mm^2, respectively. A simulated design of the bare RC structure is carried out in compliance with a former Italian building code [9], assuming: medium-risk seismic zone; typical subsoil class; strategic function after an earthquake. Geometric properties of the RC cross-section are reported in Table 1, with flat interior beams oriented parallel to the floor slab direction, while main dynamic properties are reported in Table 2 (i.e. two main vibration periods and corresponding effective masses, along the in-plan X and Y principal directions, expressed as a percentage of the corresponding total mass). Further details can be found in a previous paper [8].

Table 1: Geometric properties of RC frame members (unit in m)

Storey	Deep beams	Flat beams	Perimeter columns	Interior columns
5	0.30×0.70	0.50×0.25	0.30×0.60	0.40×0.40
4	0.30×0.75	0.50×0.25	0.30×0.70	0.50×0.50
3	0.30×0.80	0.60×0.25	0.30×0.80	0.60×0.60
2	0.30×0.85	0.60×0.25	0.30×0.90	0.70×0.70
1	0.30×0.90	0.70×0.25	0.40×0.90	0.70×0.70

Table 2: Dynamic properties of the bare structure (units in t, m and s)

m_{tot}	T_{1X}	m_{1X} (%m_{tot})	T_{1Y}	m_{1Y} (%m_{tot})
2369	0.677	75.25	0.574	74.56

Capacity curves of the bare structure along the X and Y principal directions are plotted in Figure 2, in terms of roof drift ratio (i.e. d_{top}/H_{tot}, d_{top} and H_{tot} being the horizontal top displacement and total height) versus normalised base shear (i.e. V_{base}/W_{tot},W_{tot} being the total seismic weight). Constant gravity loads are applied together with invariant distributions of lateral loads monotonically increasing and proportional to the floor masses, with (i.e. "modal") and without (i.e. "uniform") considering the contribution of the first (elastic) vibration mode. Four structural damage thresholds are considered, three in terms of inter-storey drift ratio (i.e. Δ/h=0.5%, 1% and 2%, with Δ interstorey drift and h storey height) and the last corresponding to the attainment of the ultimate value of curvature ductility demand ($\mu_{\phi u}$) at critical end sections of the frame members, evaluated in accordance with the provisions of the NTC18 for existing buildings [10].

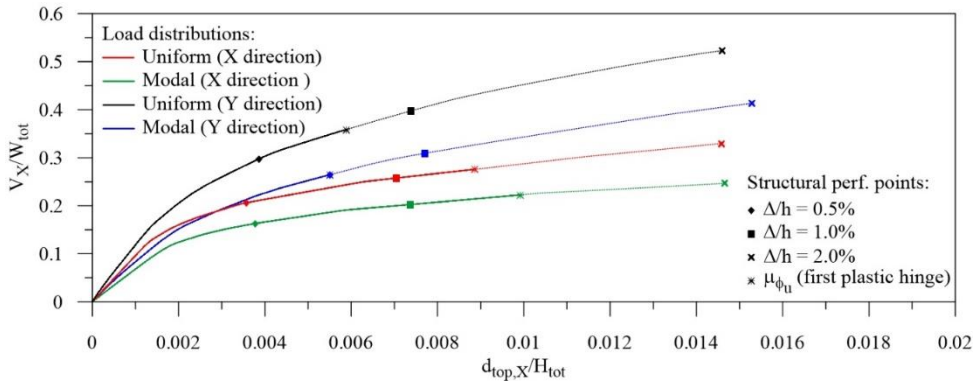

Figure 2: Capacity curves of the bare original structure

The retrofitting of the original test structure in a high-risk seismic zone (longitude 16.1852 and latitude 39.333) and considering NTC18 provisions for live loads of a hospital [8], is carried by the insertion of hysteretic dissipative exoskeletons with three in-plan arrangements parallel to the building plan: i.e. lumped (DEX.L, Figure 3), distributed (DEX.D, Figure 4) and mixed with a steel exoskeleton (MDEX.L, Figure 5). In-elevation distribution laws of lateral stiffness (i.e. $K_{i,DEX}$, for DEX, and $K_{i,EX}$, for EX) and yield shear (i.e. $V_{i,DEX}$) of the hysteretic dissipative exoskeleton are reported in Tables 3-5.

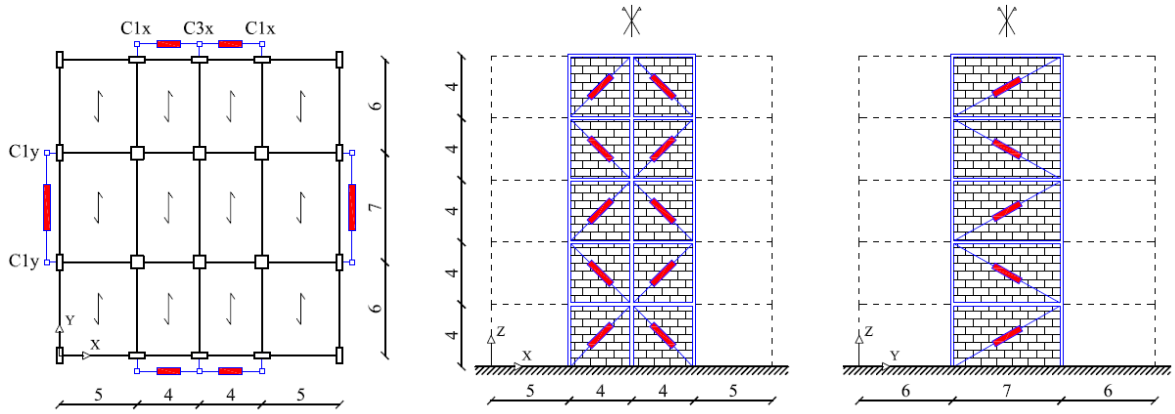

(a) Plan (X-Y) (b) Elevation (X-Z) (c) Elevation (Y-Z)

Figure 3: Layout of the hospital retrofitted with lumped dissipative exoskeleton (DEXF.L)

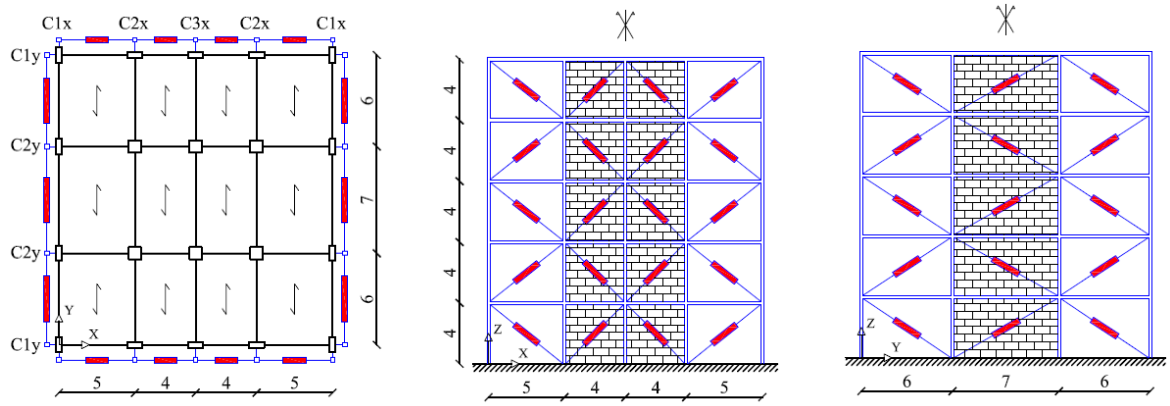

(a) Plan (X-Y) (b) Elevation (X-Z) (c) Elevation (Y-Z)

Figure 4: Layout of the hospital retrofitted with distributed dissipative exoskeleton (DEXF.D)

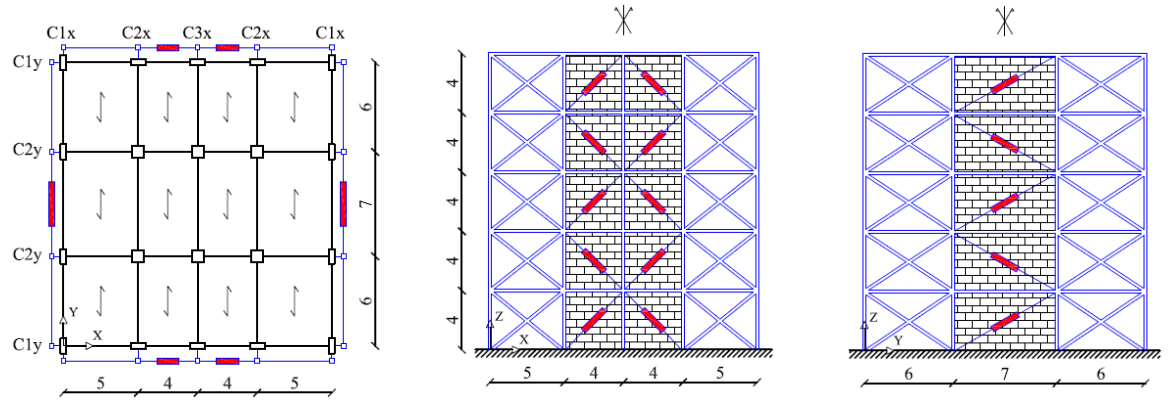

(a) Plan (X-Y) (b) Elevation (X-Z) (c) Elevation (Y-Z)

Figure 5: Layout of the hospital retrofitted with mixed DEX.L and EX (MDEXF.L)

The selected parameters of the DBD procedure of the DEXs are as follows: ductility demand of the hysteretic damped braces (HYDBs), μ_{DB}=10; hardening ratio of the hysteretic damped braces, r_{DB}=3%; ductility demand of the frame, μ_F=1.5; hardening ratio of the frame, r_F=5%.

The properties of the HYDBs are evaluated supposing that any brace is rigid enough that its deformability can be neglected (i.e. assuming $K_{DB} \cong K_D$ and $\mu_{DB} \cong \mu_D$) and assuming $\mu_{DB,u}=20$.

Table 3: Stiffness and strength properties of DEX.L and DEX.D (units in kN and m)

	DEX.L				DEX.D			
	X direction		Y direction		X direction		Y direction	
Storey	$K_{i,DEX}$	$V_{i,DEX}$	$K_{i,DEX}$	$V_{i,DEX}$	$K_{i,DEX}$	$V_{i,DEX}$	$K_{i,DEX}$	$V_{i,DEX}$
5	185729	184	480500	466	76908	92	232227	155
4	275719	398	755303	996	114171	199	365041	332
3	367754	557	1040989	1381	152281	279	503114	460
2	497032	653	1521897	1608	205813	326	735539	536
1	870536	692	2433449	1708	360476	346	1176096	569

Table 4: Stiffness and strength properties of MDEX.L for $\beta_k=0.5$ (units in kN and m)

	X direction			Y direction		
Storey	$K_{i,DEX}$	$K_{i,EX}$	$V_{i,DEX}$	$K_{i,DEX}$	$K_{i,EX}$	$V_{i,DEX}$
5	106096	53048	123	308217	154109	311
4	157502	78751	266	484490	242245	664
3	210076	105038	371	667744	333872	921
2	283925	141962	435	976223	488111	1072
1	497285	248643	461	1560939	780469	1138

Table 5: Stiffness and strength properties of MDEX.L for $\beta_k=1.0$ (units in kN and m)

	X direction			Y direction		
Storey	$K_{i,DEX}$	$K_{i,EX}$	$V_{i,DEX}$	$K_{i,DEX}$	$K_{i,EX}$	$V_{i,DEX}$
5	75752	75752	92	230332	230332	233
4	112456	112456	199	362061	362061	498
3	149994	149994	279	499007	499007	691
2	202722	202722	326	729534	729534	804
1	355061	355061	346	1166495	1166495	854

4 NUMERICAL RESULTS

The nonlinear seismic performance of the RC hospital building before and after retrofitting with hysteretic DEXs is investigated herein, assuming artificial accelerograms whose response spectra match those provided by NTC18 at the serviceability (i.e. full operational, FO, and operational, OP) and ultimate (i.e. life-safety, LS, and collapse prevention, CP) limit states [11]. A homemade computer code is implemented for nonlinear dynamic analysis of the original (F) and retrofitted (DEXF) infilled frames. Specifically, a lumped plasticity model describes the inelastic behaviour of the RC frame members and a five-element macro-model predicts the IP and OOP nonlinear mutual interaction of MIs [7, 8]. An elastic-linear behaviour is assumed for the concentric steel bracing system of the DEX, which is designed to prevent yielding in tension and buckling in compression of all members, while a bilinear force-displacement law is considered for the diagonal braces equipped with HYDs. An elastic viscous damping ratio equal to 2% is assumed for the infilled structures, in line with the Rayleigh approach.

Curves representing maximum values attained by the safety factors controlling yielding and buckling of corner (C_1), perimeter (C_2) and central (C_3) steel columns of the DEXs are reported along the in-plan X (Figure 6) and Y (Figure 7) principal directions. Specifically, tensile and compressive axial forces induced by the seismic loads at the CP limit state are divided by the corresponding tension (yielding) and compression (buckling) resisting forces calculated in line with NTC18 [10]. As can be observed, safety factors less than 1 confirm the design assumption of elastic behaviour of steel frame members. Similar results, omitted for the sake of brevity, are obtained for steel beams and diagonal braces.

The in-elevation distribution of maximum ductility demand for the HYDBs of all DEXs ($\mu_{D,max}$) is plotted in Figure 8. As can be observed, the activation of the HYDBs starts at the FO limit state, with a quite uniform distribution along the building height, while the ultimate value ($\mu_{D,u}$=20) is never reached at the LS and CP limit states, thereby preventing their collapse. The effectiveness of these retrofitting techniques is confirmed by the ductility demand of RC frame members always less than the corresponding ultimate values.

An overview of the IP and OOP collapse of MIs on the façades of the original and retrofitted hospitals is reported in Figure 9, considering the IP↔OOP mutual interaction. As shown, all DEXs are able to prevent IP collapse (see green box) observed in the original structure at the LS limit state (Figure 9c). Moreover, limited OOP collapses (see red box) are observed at the FO (Figure 9a) and OP (Figure 9b) limit states for DEXF.L and DEXF.D retrofitted structures if lower-bound OOP properties of MIs are assumed, while MDEXF.L prevents OOP collapse of MIs at all storeys for both the serviceability limit states.

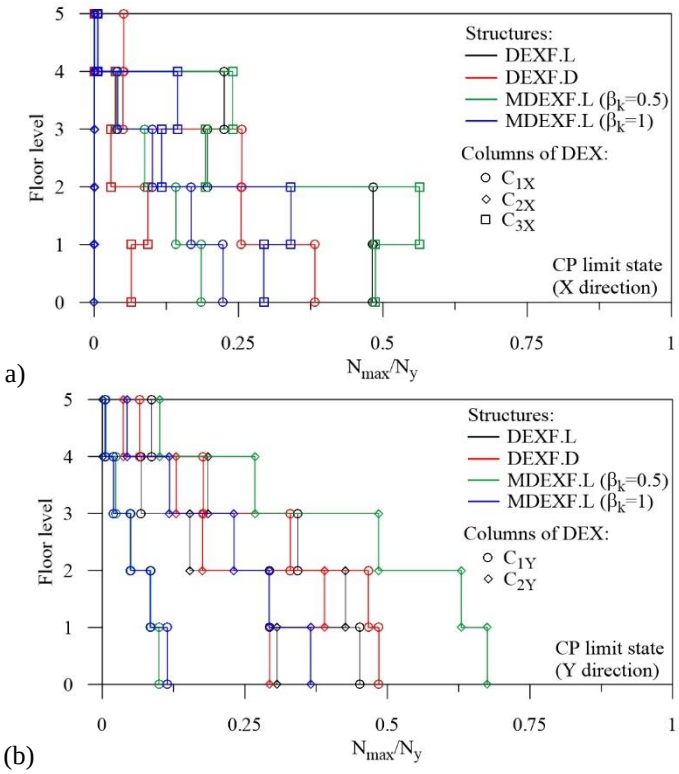

Figure 6: Safety factor against yielding for steel columns of the DEXs

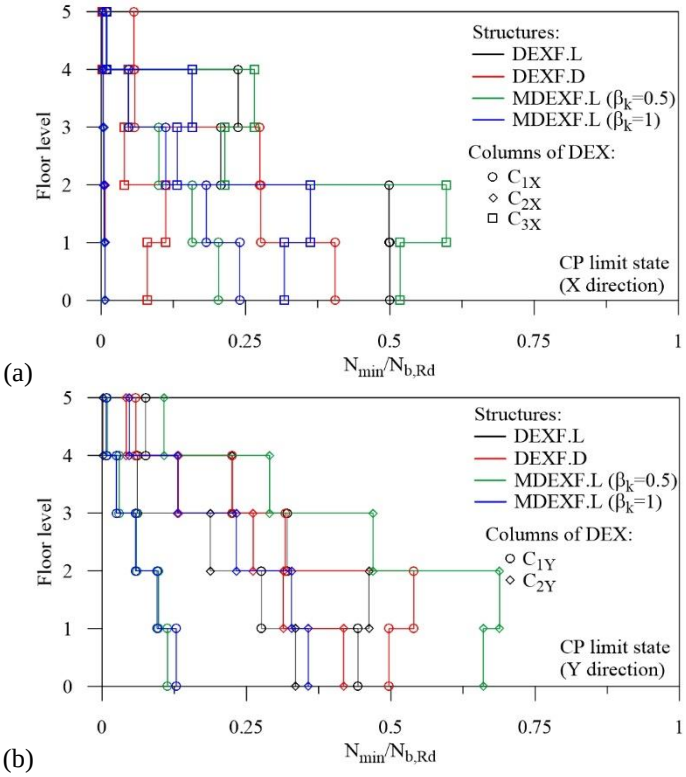

Figure 7: Safety factor against buckling for steel columns of the DEXs

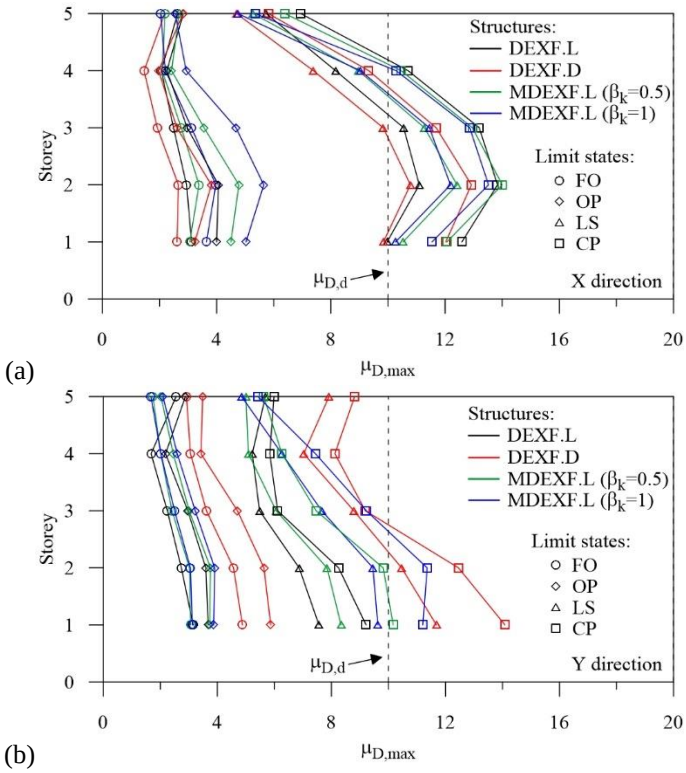

Figure 8: Ductility demand of the HYDBs

The extensive OOP collapse of MIs along the X direction at the LS limit state (Figure 9c) highlights that the insertion of the hysteretic DEXs is not always beneficial, unless upper bound OOP force-displacement laws of MIs are considered (Figure 9d) in order to take into account uncertainty about their geometrical and mechanical properties.

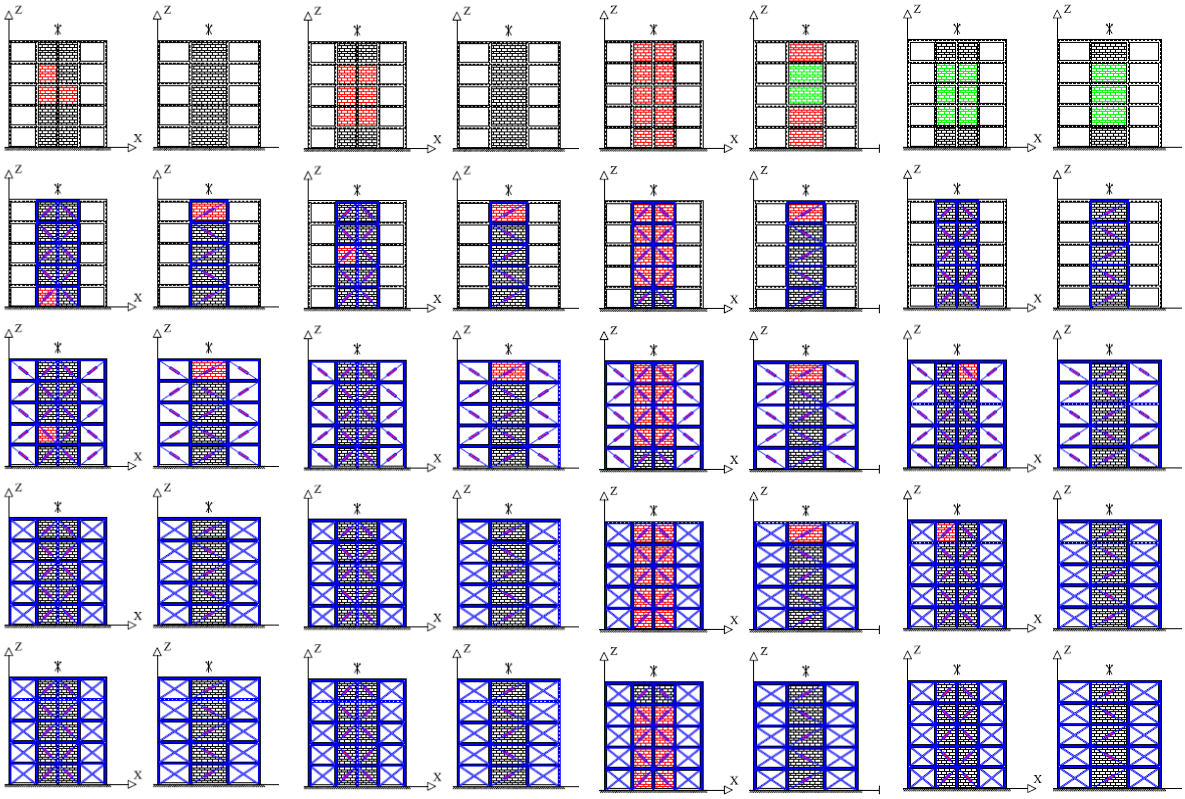

(a) FO limit state: LB (b) OP limit state: LB (c) LS limit state: LB (d) LS limit state:UB

Figure 9: In-plane (green) and out-of-plane (red) collapse mechanisms of lower-bound (LB) and upper-bound (UB) properties of MIs of the retrofitted hospital

5 CONCLUSIONS

A displacement-based seismic design procedure of dissipative steel exoskeletons is proposed herein, characterized by a rigid link at the floor levels connecting them to the existing structure and hysteretic damped braces activated by the relative displacement between adjacent floors. Three in-parallel configurations of the hysteretic DEX are considered along all façades of the perimeter of a six-storey RC building, representative of a pavilion of a hospital building located in Avellino (Italy): i.e. lumped (DEX.L), distributed (DEX.D) and mixed (MDEX.L), the latter obtained combining DEX.L with a steel exoskeleton. Results of nonlinear dynamic analysis, in terms of safety factors against yielding and buckling phenomena, confirm the reliability of the design procedure based on the assumption of elastic-linear behaviour of steel truss members. The reliability of the DEXs is resulted from the ductility demand of HYDBs at all limit states, preventing the attainment of the ultimate ductility of RC frame members. The effectiveness of DEXs for the seismic protection of MIs against the OOP collapse induced by IP-OOP nonlinear interaction is also analysed considering variability of OOP mechanical properties.

ACKNOWLEDGEMENTS

The studies presented here were carried out as part of the work envisaged by the 2024-2026 Agreement between the Italian Department of Civil Protection (DPC) and the ReLUIS Consortium.

REFERENCES

[1] Mazza, F. 2021. "Dissipative steel exoskeletons for the seismic control of reinforced concrete framed buildings Validation." Structural Control and Health Monitoring 28, no. 3: e2683. https://doi.org/10.1002/stc.2683

[2] Santarsiero, G., A. D'Angola, G. Ventura, A. Masi, V. Manfredi, V. Picciano, and A. Digrisolo. 2023. "Sustainable renovation of public buildings through seismic–energy upgrading: methodology and application to an RC school building." Infrastructures 8, no. 12: 168. https://doi.org/10.3390/infrastructures8120168

[3] Cucuzza, R., A. Aloisio, M. Domaneschi, and R. Nascimbene. 2024. "Sustainable renovation of public buildings through seismic–energy upgrading: methodology and application to an RC school building." Bulletin of Earthquake Engineering 22: 3323-3351. https://doi.org/10.1007/s10518-024-01894-0

[4] Gioiella, L., E. Tubaldi, F. Gara, L. Dezi, and A. Dall'Asta. 2018. "Modal properties and seismic behaviour of buildings equipped with external dissipative pinned rocking braced frames." Engineering Structures 172: 807-819. https://doi.org/10.1016/j.engstruct.2018.06.043

[5] Passoni, C., J. Guo, C. Christopoulos, A. Marini, and P. Riva. 2020. "Design of dissipative and elastic high-strength exoskeleton solutions for sustainable seismic upgrades of existing RC buildings." Engineering Structures 221: 111057. https://doi.org/10.1016/j.engstruct.2020.111057

[6] Prota, A., R. Tartaglia, G. Di Lorenzo, and R. Landolfo. 2024. "Seismic strengthening of isolated RC framed structures through orthogonal steel exoskeleton: bidirectional non-linear analyses." Engineering Structures 302: 117496. https://doi.org/10.1016/j.engstruct.2024.117496

[7] Mazza, F., and A. Donnici. 2021. "In-plane and out-of-plane seismic damage of masonry infills in existing r.c. structures: the case study of De Gasperi-Battaglia school in Norcia." Bulletin of Earthquake Engineering 19, no. 1: 345-376. https://doi.org/10.1007/s10518-020-00981-2

[8] Mazza, F. 2021. "In-plane and out-of-plane nonlinear seismic response of masonry infills for hospitals retrofitted with hysteretic damped braces." Soil Dynamics and Earthquake Engineering 148: 106803. https://doi.org/10.1016/j.soildyn.2021.106803

[9] DM96, Norme tecniche per le costruzioni in zone sismiche e relative istruzioni. D. M. 16-01-1996 and C.M. 10-04-1997, Italian Ministry of Public Works, Rome, Italy.

[10] NTC18, Norme tecniche per le costruzioni e relative istruzioni. D.M. 17-01-2018 and C.M. 11-02-2019, Italian Ministry of the Infrastructures and Transports, Rome, Italy.

[11] Seismoartif Seismosoft, A computer program for generation of artificial accelerograms. Available from url www.seismosoft.com; 2019.

[12] Dwairi, H.M., M.J. Kowalsky, and J.M. Nau. 2007 "Equivalent damping in support of direct displacement-based design." Journal of Earthquake Engineering 11, no. 4: 512-530. https://doi.org/10.1080/13632460601033884